THE JOURNAL OF PHYSICAL CHEMISTRY A
A JOURNAL OF THE AMERICAN CHEMICAL SOCIETY

pubs.acs.org/JPCA Article

Lewis Acid Stabilized Diatomic Molecules of Group 14: A Computational Study on $[(CO)_4Fe]_2E_2$ (E = C, Si, Ge, Sn, Pb)

Published as part of The Journal of Physical Chemistry A virtual special issue "Krishnan Raghavachari Festschrift".

Sandeep Kumar, Pattiyil Parameswaran, Anukul Jana,* and Eluvathingal D. Jemmis*

Cite This: *J. Phys. Chem. A* 2023, 127, 9442−9450 Read Online

ACCESS | Metrics & More | Article Recommendations | Supporting Information

ABSTRACT: A Lewis base and acid combination has been effectively employed to stabilize and isolate the low-valent group 14 compounds. We report DFT studies on stabilizing low-valent group 14 diatomics as adducts of Lewis acids employing transition metal carbonyl fragment iron tetracarbonyl $[Fe(CO)_4]$ as Lewis acid. Computational studies on $[(CO)_4Fe]_2E_2$, E = C, Si, Ge, Sn, and Pb, predict five plausible isomers on its potential energy surface: linear (**E2_L**), bent (**E2_B**), three-membered (**E2_T**), dibridged (**E2_D**), and four-membered (**E2_F**). For the carbon analogue, the lowest energy configuration is linear and has a typical cumulenic structure, while silicon and germanium analogues favor three-membered cyclic isomers. Four-membered cyclic isomers are the most stable for tin and lead analogues.

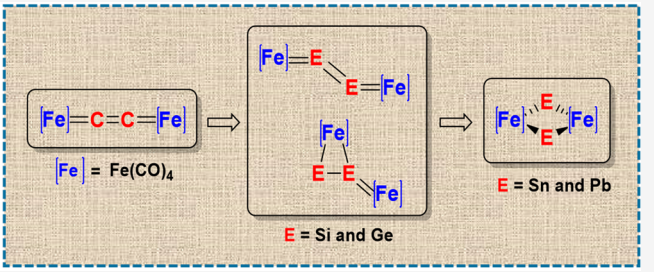

1. INTRODUCTION

Since the detection of the methylidyne radical (CH·) in interstellar medium in 1937, many highly reactive species such as monotomic carbon (C), and diatomic carbon (C_2) have been observed under similar conditions.[1−3] The extreme difficulty in synthesizing these reactive species in the laboratory encouraged theoretical studies to predict the structure and physical and chemical properties to help in their synthesis and characterization.[4,5] Chemists have been trying to overcome the kinetic instability by employing different strategies.[6−14] Our interest in generating zero oxidation state group 14 compounds stems from their relevance to materials for electronic and photovoltaic devices.[15−17] In recent years, group 14 elements in zero oxidation state have been isolated as adducts of Lewis bases such as phosphine,[18] *N*-heterocyclic carbene (NHC),[19−26] *N*-heterocyclic silylene (NHSi),[27−29] and cyclic alkyl amino carbene (CAAC)[30,31] as stabilizing ligands. The influence of π-back bonding between the ligands and low-valent center plays an important role in stabilizing this class of molecules by pulling the electron density from the low-valent center and/or moiety.[32,33]

Another way is to reduce the electron density from the donor-stabilized low-valent center by coordinating its lone pair of electrons to Lewis acids. This also potentially blocks possible oxidation reactions at that center.[34,35] We are interested in stabilizing main group elements using Lewis acids such as $Fe(CO)_4$.

A similar strategy has been successful for the isolation of β-diketiminate stabilized heteroleptic tin(II)-hydroxide **I**,[36] amidinate stabilized heteroleptic silicon(II)-hydride **II**,[37] and amidinate stabilized heteroleptic silicon(II)-fluoride **III** (Scheme 1).[38] In the case of silicon(II)-hydride **II**, it is shown that the Lewis acid undergoes an intermolecular hydrosilylation reaction in the absence of coordination with BH_3.[39] Moreover, Rivard et al. isolated heavier tetrel(II)-dihydrides **IV**,[40−45] and homo/hetero nuclear heavier parent group 14 olefins **V**[46,47] using Lewis acid and Lewis base simultaneously as stabilizing reagents. Isolation and reactions of donor−acceptor stabilized digermanium(0), $[NHC^{iPr_2Me_2}GeFe(CO)_4]_2$ ($NHC^{iPr_2Me_2}$ = 1,3-diisopropyl-4,5-dimethylimidazol-2-ylidene) is another development in the area.[48,49] Driess et al. reported the isolation of germylone **VI** using bis-NHSi as a donor and $Fe(CO)_4$ as an acceptor (Scheme 1).[50] Subsequently, in a similar strategy, stannylone and plumbylone have been reported.[51−53] In 1988, Zybill et al. isolated the HMPA-coordinated [HMPA = $(Me_2N)_3PO$] $[(CO)_4Fe{=}Si{=}Fe(CO)_4]$ with an interstitial silicon atom that can be regarded as Si(0) ligand and two $[Fe(CO)_4]$ units

Received: June 29, 2023
Revised: October 8, 2023
Accepted: October 12, 2023
Published: November 6, 2023

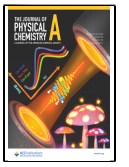

https://doi.org/10.1021/acs.jpca.3c04376
J. Phys. Chem. A 2023, 127, 9442−9450

Scheme 1. Chemical Structures of I-VI ([Fe] = $Fe(CO)_4$, [M] = $M(CO)_5$; M = Cr, Mo, and W, LA = BH_3, $W(CO)_5$)

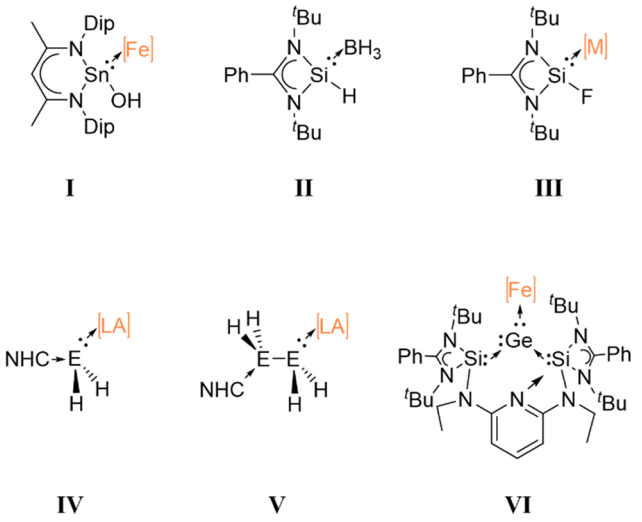

I II III IV V VI

as acceptors.[54] An analogous germanium compound $[(CO)_5W{=}Ge{=}W(CO)_5]$ was electrochemically synthesized by Budnikova et al.[55] Parameswaran and Frenking reported the theoretical calculations of naked group 14 atoms as ligands in transition-metal complexes $[(PMe_3)_2Cl_2M(E)]$ and $[(PMe_3)_2(CO)_2M(E)]$ (M = Fe, Ru, Os, and E = C−Sn) and also its complexation with $[W(CO)_5]$ leading to $[(PMe_3)_2Cl_2M{-}E{-}W(CO)_5]$ adducts.[56,57]

We are interested in stabilizing diatomic molecules of Group 14, E_2 (E = C−Pb), by an easily accessible Lewis acid, $Fe(CO)_4$.[58−60] While there has been some progress in these efforts, we report the computational studies of different isomers of $[(CO)_4Fe]_2E_2$ to assist the experimental attempts further. We have considered five isomers of $[(CO)_4Fe]_2E_2$: linear (**E2_L**), bent (**E2_B**), three-membered (**E2_T**), four-membered (**E2_F**), and dibridged (**E2_D**) structures for our study (Scheme 2) in order to plan further experiments.

Scheme 2. Chemical Structures of E2_L, E2_B, E2_T, E2_D, and E2_F (E = C−Pb) Isomers of $[(CO)_4Fe]_2E_2$

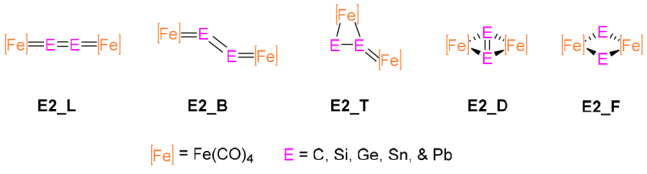

E2_L E2_B E2_T E2_D E2_F

[Fe] = $Fe(CO)_4$ E = C, Si, Ge, Sn, & Pb

2. COMPUTATIONAL DETAILS

Quantum chemical calculations are performed for geometry optimization using Gaussian 09 quantum chemistry program packages[61] to analyze thermodynamic stabilities, electronic structure, and bonding of all molecules. All the geometries are optimized employing the DFT-B3LYP functional, a combination of Becke's three-parameter hybrid exchange functional, and the Lee, Yang, Parr correlation functional.[62−65] The correlation-consistent polarized valence split basis sets cc-pVTZ for H, C, O, Si, Ge, and Fe atoms and cc-pVTZ-pp for Sn and Pb atoms are used.[66] We have also optimized Sn and Pb compounds using cc-pVTZ basis set for H, C, O, and Fe atoms and relativistic effect incorporated Stuttgart RLC-ECP basis set for Sn and Pb atoms (Table S4).[67] The effect of relativistic effects on geometrical parameters and relative energies is found to be minimal. The nature of stationary points is characterized by the Hessian matrix of force constants. The electronic energies are corrected by adding the zero-point energies for all compounds. Natural bond orbital (NBO)[68,69] analysis is performed to analyze the bonding nature with the NBO6 method at the same level of theory used for geometry optimization. The topological parameters of electron density at the bond critical points (BCPs) of E−E, E−Fe bond paths are computed using the Quantum Theory of Atoms in Molecules (QTAIM) implemented in the AIMALL program package.[70−73] The orbital evolution analysis is carried out using the intrinsic bond orbital (IBO) representation of the wave function.[74,75] The intrinsic reaction coordinate (IRC) calculation is performed utilizing the Gaussian 09 program package and the same level of theory. IBOs (*iboexp* = 2) are generated at each point of the IRC at the PBE/def2-TZVP level of theory using IboView.

3. RESULTS AND DISCUSSION

We begin with a discussion of the comparative analysis of different isomers of $[(CO)_4Fe]_2E_2$. The relative energies of the isomers and important geometrical parameters for all the structures are summarized in Tables 1−3. The variations in relative energies and geometrical parameters for the heavier analogues of carbon to lead are presented in detail in the later sections.

Table 1. Relative Energies (in kcal mol^{-1}) of Various Isomers of $[(CO)_4Fe]_2E_2$ Calculated Using the B3LYP-DFT Functional with cc-pVTZ for C, O, Si, Ge, and Fe Atoms and cc-pVTZ-pp for Sn and Pb Atoms[a]

E	E2_L	E2_B	E2_T	E2_D	E2_F
C	00.00 (0)			43.31 (0)	146.07 (0)
Si	00.00 (1)	−7.40 (0)	−10.64 (0)		2.65 (2)
Ge	00.00 (1)	−12.37 (0)	−15.49 (0)		−11.17 (1)
Sn	00.00 (1)	−17.34 (0)	−23.84 (0)		−31.78 (0)
Pb	00.00 (1)	−23.04 (0)	−29.51 (0)		−45.03 (0)

[a]No. of imaginary frequencies are given in parentheses.

Out of the five structural possibilities considered, three minima (**C2_L**, **C2_D**, and **C2_F**) are found for carbon analogue, while two minima are observed for silicon and germanium (**E2_B**, **E2_T**; E = Si, Ge), and three for the tin and lead (**E2_B**, **E2_T**, **E2_F**; E = Sn, Pb) analogues on the potential energy surface (PES). As expected, the classical linear structure, **C2_L**, is the lowest energy minimum (Table 1). The next lower-lying minimum, the dibridged structure **C2_D**, is found to be 43.31 kcal mol^{-1} higher in energy than the **C2_L**. This geometry is a stationary point only for the carbon analogue. The four-membered cyclic structure **C2_F** is the least stable isomer and has a very high relative energy of 146.07 kcal mol^{-1}.

In contrast to the carbon analogue, the linear structure **E2_L** (E = Si−Pb) is a saddle point in heavier analogues. The three-membered cyclic structure (**E2_T**) becomes the global energy minimum for silicon and germanium analogues, and the four-membered cyclic structure (**E2_F**) for tin and lead analogues (Table 1). This stability trend strongly correlates with the structural variations observed in the heavy-atom analogues of

https://doi.org/10.1021/acs.jpca.3c04376
J. Phys. Chem. A 2023, 127, 9442−9450

Table 2. Selected Bond Lengths (Å) of the Optimized Geometries of All the Isomers Calculated Using B3LYP-DFT Functional with cc-pVTZ Basis Set for C, O, Si, Ge, and Fe Atoms and cc-pVTZ-pp Basis Set for Sn and Pb Atoms

isomer	bond	C	Si	Ge	Sn	Pb
E2_L	E—E	1.264	2.150	2.262	2.638	2.783
	E—Fe	1.834	2.178	2.267	2.468	2.569
E2_B	E—E		2.260	2.408	2.843	3.030
	E—Fe		2.182	2.264	2.456	2.538
E2_T	E—E		2.331	2.468	2.853	3.008
	E1—Fe_b[a]		2.502	2.581	2.767	2.778
	E_2—Fe_b[a]		2.393	2.506	2.746	2.955
	E_2—Fe_t[a]		2.197	2.281	2.472	2.563
E2_D	E—E	1.268				
	E—Fe	2.103				
E2_F	E—E	2.378	2.837	3.079	3.497	3.642
	E—Fe	1.958	2.450	2.548	2.756	2.846

[a]Subscript b and t differentiate the bridging and terminal Fe in the **E2_T** isomer.

Table 3. Selected Bond Angles (deg) of the Optimized Geometries of All the Isomers Calculated Using B3LYP-DFT Functional with cc-pVTZ Basis Set for C, O, Si, Ge, and Fe Atoms and cc-pVTZ-pp Basis Set for Sn and Pb Atoms

isomer	bond angle	C	Si	Ge	Sn	Pb
E2_L	E—E—Fe	180.0	180.0	180.0	180.0	180.0
E2_B	E—E—Fe		140.0	136.4	133.3	132.6
E2_T	E_1—Fe_b—E_2[a]		56.8	58.0	62.3	63.2
	E_1—E_2—Fe_t[a]		150.9	155.2	164.6	178.0
E2_D	E—Fe—E	35.1				
E2_F	E—Fe—E	74.8	70.7	74.3	78.8	79.6
	Fe—E—Fe	105.2	109.3	105.7	101.2	100.4

[a]Subscript b and t differentiate the bridging and terminal Fe in the **E2_T** isomer.

acetylene, HEEH,[76−80] and ethylene, H_2EEH_2.[81] Among the isomers of HEEH (E = Si−Pb), it is known that the unconventional nonplanar doubly bridged, planar singly bridged, and trans-bent structures are energetically preferred compared to the conventional linear acetylene-like structure.

We have calculated the force constants of the E−E bonds in E_2 and all Lewis acid stabilized isomers of $[(CO)_4Fe]_2E_2$ (Table S6) to understand the intrinsic strength of E−E bonds. The force constant for the E−E bond in E_2 reduces as the group 14 element changes from C (12.39 mdyn $Å^{-1}$) to Pb (1.05 mdyn $Å^{-1}$), indicating the weakening of the heavier E−E bond. Interestingly, the force constants for the C−C bond slightly reduce on complexation with $Fe(CO)_4$. On the other hand, the Lewis acid complexation increases the force constant for the heavier E−E (E = Si−Pb) bonds. Hence, it can be proposed that the complexation with $Fe(CO)_4$ stabilizes the heavier diatomic molecules as compared to the corresponding carbon counterpart. In general, the force constant of the E−Fe bond (E = Si−Pb) in the bent isomer **E2_B** is higher than that of the linear isomer **E2_L**, indicating the intrinsic tendency of the linear molecule to undergo structural distortion to the bent geometry **E2_B**.

3.1. $[(CO)_4Fe]_2C_2$ Isomers. The C_2 molecule in **C2_L** is trapped between two $Fe(CO)_4$ fragments in such a way that each carbon atom binds as a vinylidene type ligand (Scheme 2). The C−C bond distance (1.264 Å) is in the range of in-between double and triple bond lengths, with a Wiberg Bond Index (WBI) of 2.256 (Table S2 SI). The middle C−C bond distance in the optimized geometry of cumulene (Figure 1) is

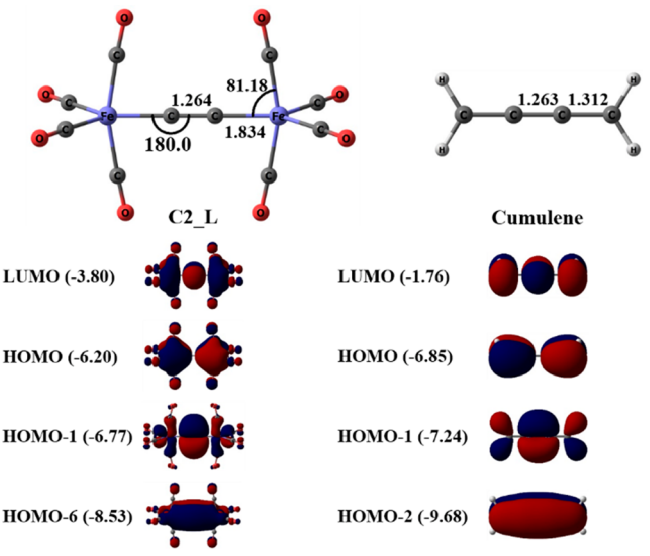

Figure 1. Optimized geometries and the corresponding plot of the frontier valence orbitals (isosurface value = 0.03) of **C2_L** and C_4H_4 at B3LYP/cc-pVTZ level (distances [Å], angles [deg]).

1.263 Å at the B3LYP/cc-pVTZ level, which is in good agreement with the C−C bond length of the **C2_L** molecule. $Fe(CO)_4$ is isolobal to CH_2, making **C2_L** a cumulene equivalent. Accordingly, the frontier molecular orbitals (FMOs) of **C2_L** and cumulene are comparable (Figure 1). Minor interactions between the π-bonding MOs of the central diatomic moiety and the π-antibonding MOs of the axial CO group are observed. These stabilizing interactions result in a slight bending of the axial carbonyl groups (Table S3, SI) toward C_2, leading to an OC−Fe−CC bond angle of 81.2° in the **C2_L** structure.

In the dibridged structure, **C2_D**, the C_2 molecule is trapped between two $Fe(CO)_4$ fragments in such a way that two carbon atoms are at the bridging position and the C−C bond is aligning perpendicular to the axial CO groups (Figure 2). The C−C bond length is 1.268 Å, which suggests a multiple bond character, and the WBI for the same is 2.212 (Table S2 SI). The bonding orbital, HOMO-2, constitutes the C−C σ-bond, and the HOMO is mainly a C−C π-bonding orbital, supporting the double bond character (Figure 3).

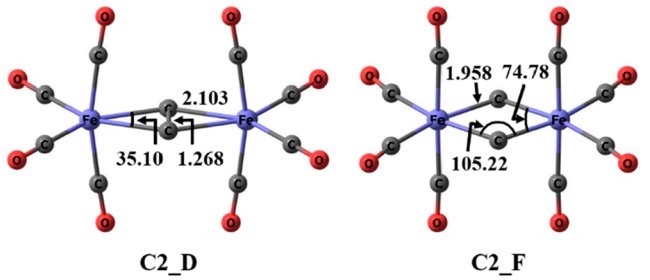

Figure 2. Optimized geometries of isomers **C2_D** and **C2_F** at B3LYP/cc-pVTZ level (distances [Å], angles [deg]).

https://doi.org/10.1021/acs.jpca.3c04376
J. Phys. Chem. A 2023, 127, 9442−9450

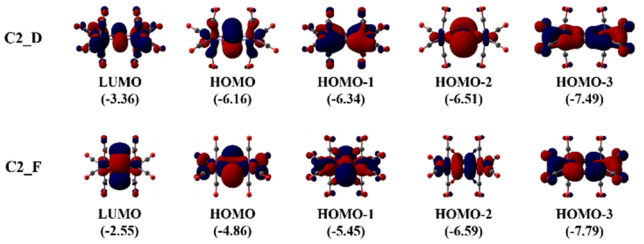

Figure 3. Plot of the frontier valence orbitals (isosurface value = 0.03) of **C2_D** and **C2_F** isomers calculated at B3LYP/cc-pVTZ level. The eigenvalues [eV] are given in parentheses.

The four-membered cyclic structure, **C2_F**, is derived from the dibridged structure, **C2_D**, by stretching the C−C bond up to a distance where there is no bonding interaction between two carbon atoms of the C_2 molecule. Each bridging C atom bears a lone pair of electrons and coordinates two Fe atoms. The structure has a planar cyclic rhomboid Fe_2C_2 core. Geometry at the Fe atom is a distorted octahedron formed by four carbonyl groups and two carbon atoms of the C_2 moiety. The distance between two carbon atoms is 2.378 Å which, is greater than the range of C−C single bond length.[82]

Molecular orbital analysis reveals a significant transformation in the nature of frontier molecular orbitals (FMOs) along the IRC scan as the geometry evolves from **C2_D** to **C2_F** (Figure S2 SI). Notably, an energy level crossing is observed between HOMO, LUMO, and LUMO+1. Specifically, the HOMO, a π-bonding orbital in the **C2_D** structure, transforms into the vacant LUMO+1 orbital in the **C2_F** structure and does not contribute to C−C π-bond. Conversely, the LUMO in **C2_D**, initially a σ-antibonding orbital, transforms into the HOMO, which is an antibonding combination of the σ lone-pair orbitals at the carbon atoms. Additionally, the transformation of the HOMO-2, a σ-bonding orbital, results in the formation of HOMO-1, which is a bonding combination of the σ lone-pair orbitals at the carbon atoms. IBO analysis shows the evolution of the localized orbitals along the IRC path (Figures S3 and S4 SI). The C−C σ-bonding localized orbital transforms into the two carbon-centered lone-pair orbitals, while the π-bonding localized orbital transforms into a virtual bonding π-orbital. A shift in the electron pairs responsible for C−C bonding toward the nonbonding lone pairs is obvious here. The absence of a C−C bond and the presence of a lone pair on each carbon atom contributes to the high instability exhibited by the **C2_F** isomer.

3.2. E2_L (E = Si−Pb) Isomers: Heavier Analogues of Linear Structures. Drawing a direct structural comparison with the heavy-atom analogues of acetylene,[76−80] we expect the linear isomer **E2_L** (E = Si−Pb) to be a first-order saddle point on its PES. Geometry optimization of the **E2_L** structure leads to a transition state (TS). The Hessian matrix analysis reveals a single imaginary frequency associated with the in-plane bending motion of two $Fe(CO)_4$ groups in trans-bent conformation. The magnitude of imaginary frequencies are 108.56 cm^{-1} for Si, 99.67 cm^{-1} for Ge, 92.65 cm^{-1} for Sn, and 104.09 cm^{-1} for Pb. The relative energies of **E2_L** isomers increase with respect to **E2_T** when the E atom becomes heavier: 10.64 kcal mol^{-1} for Si, 15.49 kcal mol^{-1} for Ge, 23.84 kcal mol^{-1} for Sn, and 29.51 kcal mol^{-1} for Pb (Table 1). This happens because the ability of heavier atoms to form π-bond in E_2 moiety decreases due to poor overlap of p-orbitals.[83,84]

3.3. E2_B (E = Si−Pb) Isomers: Bent Structures. The geometry optimization of structure **E2_B** (E = Si−Pb) leads to a minimum energy structure on its PES (Figure 4). Two

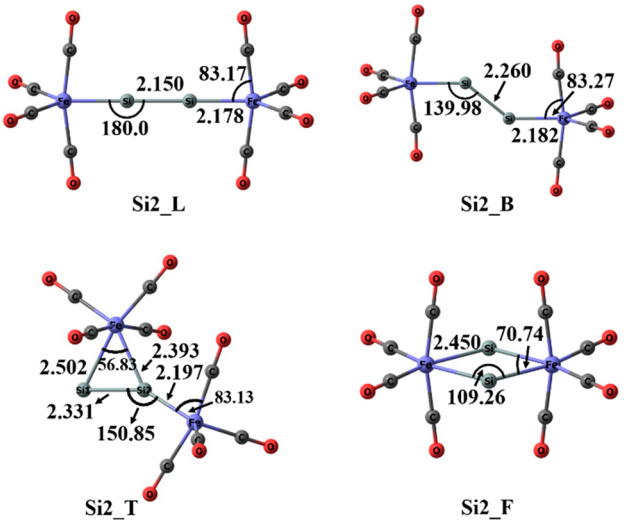

Figure 4. Optimized geometries of **Si2_L**, **Si2_B**, **Si2_T**, and **Si2_F** isomers at B3LYP/cc-pVTZ level (distances [Å], angles [deg]). Geometries of heavier analogues (E = Ge, Sn, and Pb) are similar to their respective Si complexes (Figure S1 SI).

$[Fe(CO)_4]$ units are in-plane trans-bent with E−E−Fe bond angles of 140.0° (Si), 136.4° (Ge), 133.3° (Sn), and 132.6° (Pb) (Table 3). The E−E bond length, viz., 2.260 Å (Si), 2.408 Å (Ge), 2.843 Å (Sn), and 3.030 Å (Pb) are within the reported range of disilenes, digermenes, distannenes, and diplumbenes, respectively.[85] The relative energies of **E2_B** isomers with respect to **E2_T** follow an overall increasing trend as E becomes heavier: 3.24 kcal mol^{-1} for Si, 3.12 kcal mol^{-1} for Ge, 6.50 kcal mol^{-1} for Sn, and 6.47 kcal mol^{-1} for Pb (Table 1).

HOMO is an in-plane π-bonding orbital, and LUMO is an out-of-plane π-bonding orbital with an antibonding combination with d-orbital of $Fe(CO)_4$ fragments in **E2_L** isomer (Figure 5). Upon the bending of two $Fe(CO)_4$ fragments, the weak in-plane π-bonding molecular orbital undergoes rehybridization and generates some nonbonding character. This HOMO is stabilized with increased bonding interaction with

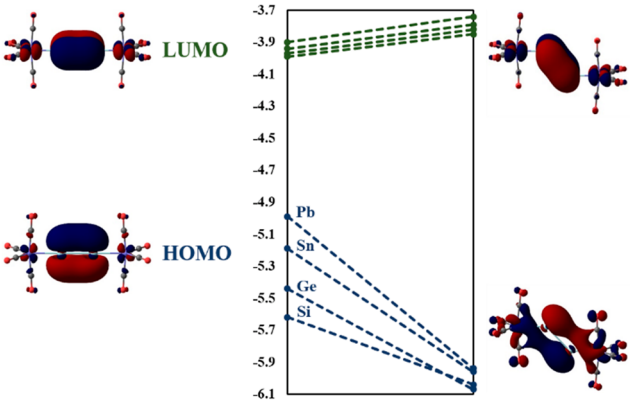

Figure 5. MO correlation diagram for HOMO and LUMO in bending of $Fe(CO)_4$ fragments from **E2_L** to **E2_B** isomer.

https://doi.org/10.1021/acs.jpca.3c04376
J. Phys. Chem. A 2023, 127, 9442−9450

Table 4. Topological Parameters (a.u.) at Bond Critical Points (BCPs) for E−E and E−Fe (E = C−Pb) Bonds of All the Structures Using Quantum Theory of Atoms in Molecules (QTAIM)[a]

Isomer	Bond	$\rho(r)$	$\nabla^2\rho(r)$	$V(r)$	$G(r)$	$H(r) = V(r) + G(r)$	$H(r)/\rho(r)$
C2_L	C−C	0.401	−1.497	−0.799	0.213	−0.587	−1.465
	C−Fe	0.145	0.328	−0.219	0.151	−0.069	−0.473
C2_D	C−C	0.423	−1.632	−0.837	0.215	−0.622	−1.473
	C−Fe	0.080	0.260	−0.108	0.087	−0.022	−0.272
C2_F	C−Fe	0.124	0.124	−0.140	0.085	−0.054	−0.440
Si2_L	Si−Si	0.101	−0.141	−0.086	0.025	−0.060	−0.596
	Si−Fe	0.086	−0.004	−0.089	0.044	−0.045	−0.521
Si2_B	Si−Si	0.090	−0.117	−0.065	0.018	−0.047	−0.526
	Si−Fe	0.088	−0.022	−0.088	0.042	−0.047	−0.533
Si2_T	Si−Si	0.087	−0.113	−0.060	0.016	−0.044	−0.505
	Si_1−Fe_b	0.059	0.002	−0.041	0.020	−0.020	−0.339
	Si_2−Fe_b	0.067	−0.001	−0.053	0.026	−0.027	−0.393
	Si_2−Fe_t	0.087	−0.014	−0.086	0.041	−0.045	−0.516
Si2_F	Si−Fe	0.064	−0.007	−0.045	0.022	−0.024	−0.370
Ge2_L	Ge−Ge	0.092	−0.018	−0.080	0.038	−0.043	−0.462
	Ge−Fe	0.078	0.095	−0.086	0.055	−0.031	−0.396
Ge2_B	Ge−Ge	0.075	−0.013	−0.053	0.025	−0.028	−0.378
	Ge−Fe	0.082	0.0761	−0.087	0.053	−0.034	−0.413
Ge2_T	Ge−Ge	0.072	−0.020	−0.047	0.021	−0.026	−0.360
	Ge_1−Fe_b	0.053	0.023	−0.035	0.020	−0.015	−0.275
	Ge_2−Fe_b	0.058	0.036	−0.043	0.026	−0.017	−0.295
	Ge_2−Fe_t	0.079	0.080	−0.082	0.051	−0.031	−0.396
Ge2_F	Ge−Fe	0.056	0.022	−0.038	0.022	−0.016	−0.289
Sn2_L	Sn−Sn	0.065	0.022	−0.052	0.029	−0.023	−0.352
	Sn−Fe	0.063	0.090	−0.064	0.043	−0.021	−0.334
Sn2_B	Sn−Sn	0.049	0.015	−0.030	0.017	−0.013	−0.273
	Sn−Fe	0.067	0.077	−0.067	0.043	−0.024	−0.354
Sn2_T	Sn−Sn	0.050	0.008	−0.030	0.016	−0.014	−0.282
	Sn_1−Fe_b	0.045	0.021	−0.028	0.017	−0.011	−0.252
	Sn_2−Fe_b	0.045	0.029	−0.030	0.019	−0.011	−0.249
	Sn_2−Fe_t	0.064	0.080	−0.064	0.042	−0.022	−0.340
Sn2_F	Sn−Fe	0.046	0.021	−0.028	0.017	−0.012	−0.255
Pb2_L	Pb−Pb	0.058	0.063	−0.047	0.031	−0.015	−0.262
	Pb−Fe	0.055	0.108	−0.057	0.042	−0.015	−0.274
Pb2_B	Pb−Pb	0.039	0.042	−0.024	0.017	−0.007	−0.174
	Pb−Fe	0.063	0.098	−0.063	0.044	−0.019	−0.306
Pb2_T	Pb−Pb	0.042	0.037	−0.026	0.018	−0.008	−0.197
	Pb_1−Fe_b	0.046	0.036	−0.031	0.020	−0.011	−0.238
	Pb_2−Fe_b	0.035	0.033	−0.020	0.014	−0.006	−0.173
	Pb_2−Fe_t	0.058	0.101	−0.059	0.042	−0.017	−0.287
Pb2_F	Pb−Fe	0.041	0.031	−0.026	0.017	−0.009	−0.213

[a]Electron density ($\rho(r)$), Laplacian of electron density ($\nabla^2\rho(r)$), potential energy density ($V(r)$), kinetic energy density ($G(r)$), and total electron energy density ($H(r)$) are computed. DFT-B3LYP functional with cc-pVTZ basis set for C, O, Si, Ge, and Fe atoms and cc-pVTZ-pp basis set for Sn and Pb atoms is utilized to generate the wave function files. All the parameters are presented up to six decimal points in Table S5 (SI).

the *d*-orbital of the Fe metal atom (Figure 5). The bending of $Fe(CO)_4$ units and the stabilization of HOMO increase from Si to Pb. The stabilization of the HOMO (9.67, 14.53, 17.56, and 21.91 kcal mol^{-1}, Si−Pb, see Figure S5 SI) mirrors the corresponding total energy differences from Table 1 of 7.40, 12.37, 17.34, and 23.04 kcal mol^{-1}. This process resembles the stabilization mechanism observed in heavy-atom analogues of acetylene and ethylene, where the trans-bending of hydrogen atoms within the linear structures plays a pivotal role in achieving a more stable conformation and lowering its energy on the PES landscape. The peculiarity in the trans-bent geometries of the heavy analogues can be attributed to the stabilization of valence s-electrons as group 14 element changes from C to Pb and, as a result, the lower involvement of valence s-electrons toward bonding.[76−81]

3.4. E2_T (E = Si−Pb) Isomers: Three-Membered Cyclic Structures. The geometry optimization of structure **E2_T** (E = Si−Pb) leads to minimum energy structures on their PES for all of them (Figure 4). This isomer is a global minimum for the Si and Ge analogues and the second lowest-lying structure in the case of the Sn and Pb analogues (Table 1). The Si−Si bond length of 2.331 Å with a WBI of 0.998 indicates the Si−Si single bond character in the **Si2_T** isomer. LUMO, an out-of-plane Si−Si π-bonding orbital, supports the absence of the Si−Si double bond (Figure S6 SI). The Ge−Ge bond length in **Ge2_T** isomer is 2.468 Å, which is very close to the Ge−Ge bond distance (2.4442(2) Å) in [$NHC^{iPr_2Me_2}$GeFe-

https://doi.org/10.1021/acs.jpca.3c04376
J. Phys. Chem. A 2023, 127, 9442−9450

$(CO)_4]_2$ ($NHC^{iPr_2Me_2}$ = 1,3-diisopropyl-4,5-dimethylimidazol-2-ylidene).[48] Localized orbitals from NBO analysis (Figure S7 SI) show that there is a lone-pair orbital on the E_1 atom having occupancies of 83.74% *s*, 16.18% *p*, and 0.08% *d* orbitals in the Si analogue. The occupancies of the *s*-orbital increase from Si to Pb (Table S1 SI). The lone pair becomes more stable at heavier atoms as the *s*-orbital does not take part in bonding due to the inert pair effect. As a result of this, the stability of the **E2_T** isomers increases down the group from Si to Pb. Terminal $Fe(CO)_4$ group bending decreases down the group with an $E_1-E_2-Fe_t$ bond angle of 150.9° for Si, 155.2° for Ge, 164.6° for Sn, and 178.0° for Pb analogue. **Pb2_T** structure features Pb and Fe_t atoms in an almost linear chain (Figure S8 SI). A decrease in the bending of the terminal $Fe(CO)_4$ group increases the in-plane structural distortion in the E_2Fe three-membered ring of **E2_T** isomers. This is the likely reason for the less increase in the stability of Sn and Pb analogues, and they become the second most stable structures when compared to their counterparts **E2_F**.

3.5. E2_F (E = Si−Pb) Isomers: Four-Membered Cyclic Structures. The four-membered ring structure is a second-order stationary point for Si and a transition state for Ge. Considering various factors, such as the preference for an E−Fe−E angle of 90° for an octahedral complex and a sufficiently long nonbonded E−E distance, there is only a small window of possibility for stable structures. With E−Fe−E angles of 78.8° and 79.6° and Fe−E−Fe angles of 101.2° and 100.4°, respectively, for Sn and Pb, these structures are the lowest energy minima among the isomers considered here. There is no bonding interaction between the two E atoms in the **E2_F** structures. Each E atom bears a lone pair of electrons and forms a σ-bond with each Fe atom. The interatomic distance between two Si atoms in the **Si2_F** isomer is 2.837 Å (Table 2), which is greater than the reported Si−Si single bond lengths.[86] HOMO−1 and HOMO are the plus and minus combination of the σ lone-pair orbitals at E atoms (Figure S6 SI). NBO localized orbitals (Figure S9 SI) clearly show a lone-pair orbital of mainly *s* character on each E atom having occupancies of 83.74% *s*, 16.18% *p*, and 0.08% *d* orbitals in the Si analogue. The ability of the *s*-orbital to take part in bonding decreases down the group, leading to higher stability of the lone-pair. It is also reflected in the increase of *s*-orbital occupancies to 86.38% for Ge, 89.76% for Sn, and 92.54% for Pb (Table S1 SI). The relative energy of each isomer with respect to **E2_T** decreases down the group from Si to Pb analogue (Table 1). Silicon analogue, **Si2_F**, is the least stable structure among its isomers, being 13.29 kcal mol^{-1} (Table 1) higher in energy than its global minima, **Si2_T**. It is a second-order saddle point on the PES and displays two small imaginary frequencies of 25.00 cm^{-1} and 23.32 cm^{-1}. The germanium analogue, **Ge2_F**, is a TS that displays one imaginary frequency of 11.79 cm^{-1}. It is 4.32 kcal mol^{-1} (Table 1) higher in energy than the global minima, **Ge2_T**. The imaginary frequency in **Ge2_F** corresponds to the in-plane bending motion of two $Fe(CO)_4$ fragments. The relative energies of **E2_F** isomers with respect to **E2_T** decrease as E becomes heavier, finally making Sn and Pb analogues, **Sn2_F** and **Pb2_F**, the most stable structures among their respective isomers. This happens due to the increased stability of the lone pair of electrons as the group 14 element changes from C to Pb.

3.6. QTAIM Analysis. The topological parameters of electron density are calculated at the BCPs of E−E and E−Fe bonds of all compounds (Table 4 and Table S5). The electron density $\rho(r)$ calculated at the BCPs of the E−E bonds is found to be high and decreases as E changes from C to Pb for a particular geometry. The Laplacian of electron density $\nabla^2\rho(r)$ is negative for C, Si, and Ge compounds and slightly positive for Sn and Pb. The $\rho(r)$ and $\nabla^2\rho(r)$ values indicate that the E−E bond can be described by covalent bonding, and the covalency decreases as E becomes a heavier group 14 element. In all the compounds, the total energy density $H(r)$ at the E−E bond is found to be negative, suggesting that the E−E bond can be best described by covalent bonding interaction. To understand the relative degree of covalency, we have calculated $H(r)/\rho(r)$ at the BCPs of the E−E bonds of all compounds.[70−73] The negative $H(r)/\rho(r)$ at the BCP indicates the covalent nature of the bond, and its absolute value provides the degree of covalency. The degree of covalency decreases for a particular geometry as the group 14 element changes from C to Pb. The covalent character of the E−E bond is higher in linear geometries as compared to that in other geometries, except for the doubly bridged carbon compound **C2_D**, where the C−C bond has a slightly higher covalent character than that in the linear compound **C2_L**.

In corroboration with the electronegativity difference between E (C, 2.55; Si, 1.90; Ge, 2.01; Sn, 1.88; Pb, 2.10) and Fe (1.90), $\nabla^2\rho(r)$ at the BCP of E−Fe bond is positive for all E−Fe bonds except for E = Si, suggesting a more polar nature of E−Fe bonds (E = C, Ge, Sn, and Pb). In general, the total energy density is negative, having a smaller magnitude for all E−Fe bonds, indicating their polar covalent nature. As expected, the degree of covalency ($H(r)/\rho(r)$) of E−Fe bonds is less than that of E−E bonds.

4. CONCLUSION

Isomers of Lewis acid stabilized group 14 diatomics, $[(CO)_4Fe]_2E_2$ (E = C−Pb), are studied using DFT computations. A linear isomer is lowest in energy for the carbon analogue. In contrast, silicon and germanium analogues favor a three-membered cyclic structure **E2_T**, where one of the $Fe(CO)_4$ unit bridges the E_2 unit, and the other is attached as a terminal ligand to E_2. The tin and lead analogues prefer a four-membered cyclic structure **E2_F**. A dibridged structure is observed as a minimum only for the carbon analogue. The relative thermodynamic stability follows a trend of decreasing stability for linear, bent, and three-membered cyclic isomers. In contrast, four-membered cyclic isomers become increasingly stable as we descend down the group from carbon to lead. The QTAIM analysis indicates a higher degree of covalency for both the E−E and E−Fe (E = C−Pb) bonds, which relatively decreases in the heavy atom analogues. Efforts to develop new approaches toward experimentally evidencing diatomic molecules of group 14 elements stabilized using only Lewis acids will be rewarding.

■ ASSOCIATED CONTENT

Supporting Information

The Supporting Information is available free of charge at https://pubs.acs.org/doi/10.1021/acs.jpca.3c04376.

Figure for the optimized geometries of **E2_L**, **E2_B**, **E2_T**, and **E2_F** (E = Ge−Pb) structures, Walsh diagram, IRC scan plot, and C−C σ and π-localized IBO plot for the transformation of **C2_B** into **C2_F**, MO correlation diagram for the transformation of **E2_L** into

https://doi.org/10.1021/acs.jpca.3c04376
J. Phys. Chem. A 2023, 127, 9442−9450

E2_B (E = Si−Pb) structure, figures for the molecular orbitals, plots for localized lone-pair NBOs and table for AO contribution to NBOs of **E2_T** and **E2_F** (E = Si−Pb) structures, figure for the bending of terminal $Fe(CO)_4$ group in the **E2_T** structure, WBI table of **C2_B**, **E2_T**, and **E2_F** (E = Si−Pb) structures, table for bond angles measuring the axial CO bending, table for relative energies of Sn and Pb isomers calculated with the relativistic effects incorporated basis set, table for topological properties at BCPs, table for force constants, and the Cartesian coordinates of the studied molecules (PDF)

AUTHOR INFORMATION

Corresponding Authors

Anukul Jana − *Tata Institute of Fundamental Research Hyderabad, Hyderabad 500107 Telangana, India;* orcid.org/0000-0002-1657-1321; Email: ajana@tifr.res.in

Eluvathingal D. Jemmis − *Inorganic and Physical Chemistry Department, Indian Institute of Science, Bangalore 560012, India;* orcid.org/0000-0001-8235-3413; Email: jemmis@iisc.ac.in

Authors

Sandeep Kumar − *Inorganic and Physical Chemistry Department, Indian Institute of Science, Bangalore 560012, India*

Pattiyil Parameswaran − *Department of Chemistry, National Institute of Technology Calicut, Kozhikode 673601 Kerala, India;* orcid.org/0000-0003-2065-2463

Complete contact information is available at: https://pubs.acs.org/10.1021/acs.jpca.3c04376

Notes

The authors declare no competing financial interest.

ACKNOWLEDGMENTS

This work is supported by the Tata Institute of Fundamental Research Hyderabad, Hyderabad, India, SERB-DST (EMR/2014/001237), and CSIR-HRDG (01(2863)/16/EMR-II). We thank the Supercomputer Education and Research Centre, IISc, for the computational facilities. S.K. thanks IISc for the research fellowship. E.D.J. thanks SERB-DST for funding through the Year of Science Chair Professorship.

REFERENCES

(1) Swings, P.; Rosenfeld, L. Considerations Regarding Interstellar Molecules. *Ap. J.* **1937**, *86*, 483−486.

(2) White, G. J.; Padman, R. Images of Atomic Carbon in the Interstellar Medium. *Nature* **1991**, *354*, 511−513.

(3) Souza, S. P.; Lutz, B. L. Detection of C_2 in the Interstellar Spectrum of Cygnus OB2 Number 12 (VI Cygni Number 12)*. *Ap. J.* **1977**, *216*, L49−L51.

(4) Xu, J.; Ding, Y.-H.; Andrada, D. M.; Frenking, G. Silavinylidene Stabilized by an N-Heterocyclic Carbene: A Theoretically Predicted Stable Molecule. *Chem. Eur. J.* **2014**, *20*, 9216−9220.

(5) Andrada, D. M.; Frenking, G. Stabilization of Heterodiatomic SiC through Ligand Donation: Theoretical Investigation of $SiC(L)_2$ (L = NHC^{Me}, $CAAC^{Me}$, PMe_3). *Angew. Chem., Int. Ed.* **2015**, *54*, 12319−12324.

(6) Ghadwal, R. S.; Roesky, H. W.; Merkel, S.; Henn, J.; Stalke, D. Lewis Base Stabilized Dichlorosilylene. *Angew. Chem., Int. Ed.* **2009**, *48*, 5683−5686.

(7) Filippou, A. C.; Chernov, O.; Schnakenburg, G. $SiBr_2$(Idipp): A Stable N-Heterocyclic Carbene Adduct of Dibromosilylene. *Angew. Chem., Int. Ed.* **2009**, *48*, 5687−5690.

(8) Jana, A.; Huch, V.; Scheschkewitz, D. NHC-Stabilized Silagermenylidene: A Heavier Analogue of Vinylidene. *Angew. Chem., Int. Ed.* **2013**, *52*, 12179−12182.

(9) Jana, A.; Majumdar, M.; Huch, V.; Zimmer, M.; Scheschkewitz, D. NHC-Coordinated Silagermenylidene Functionalized in Allylic Position and Its Behaviour as a Ligand. *Dalton Trans.* **2014**, *43*, 5175−5181.

(10) Ghana, P.; Arz, M. I.; Das, U.; Schnakenburg, G.; Filippou, A. C. Si = Si double bonds: Synthesis of an NHC-stabilized disilavinylidene. *Angew. Chem., Int. Ed.* **2015**, *54*, 9980−9985.

(11) Jana, A.; Omlor, I.; Huch, V.; Rzepa, H. S.; Scheschkewitz, D. N-Heterocyclic Carbene Coordinated Neutral and Cationic Heavier Cyclopropylidenes. *Angew. Chem., Int. Ed.* **2014**, *53*, 9953−9956.

(12) Rit, A.; Campos, J.; Niu, H.; Aldridge, S. A Stable Heavier Group 14 Analogue of Vinylidene. *Nat. Chem.* **2016**, *8*, 1022−1026.

(13) Scheschkewitz, D. Organometallic Chemistry: Heavyweight Isomer Brings Stability. *Nat. Chem.* **2016**, *8*, 993−995.

(14) Transue, W. J.; Velian, A.; Nava, M.; Martin-Drumel, M.-A.; Womack, C. C.; Jiang, J.; Hou, G.-L.; Wang, X.-B.; McCarthy, M. C.; Field, R. W.; et al. A Molecular Precursor to Phosphaethyne and Its Application in Synthesis of the Aromatic 1,2,3,4-Phosphatriazolate Anion. *J. Am. Chem. Soc.* **2016**, *138*, 6731−6734.

(15) Zhao, Z.; Tian, F.; Dong, X.; Li, Q.; Wang, Q.; Wang, H.; Zhong, X.; Xu, B.; Yu, D.; He, J.; et al. Tetragonal Allotrope of Group 14 Elements. *J. Am. Chem. Soc.* **2012**, *134*, 12362−12365.

(16) Wang, Q.; Xu, B.; Sun, J.; Liu, H.; Zhao, Z.; Yu, D.; Fan, C.; He, J. Direct Band Gap Silicon Allotropes. *J. Am. Chem. Soc.* **2014**, *136*, 9826−9829.

(17) Wippermann, S.; He, Y.; Vörös, M.; Galli, G. Novel Silicon Phases and Nanostructures for Solar Energy Conversion. *Appl. Phys. Rev.* **2016**, *3*, No. 040807.

(18) Tonner, R.; Öxler, F.; Neumüller, B.; Petz, W.; Frenking, G. Carbodiphosphoranes: The Chemistry of Divalent Carbon(0). *Angew. Chem., Int. Ed.* **2006**, *45*, 8038−8042.

(19) Tonner, R.; Frenking, G. $C(NHC)_2$: Divalent Carbon(0) Compounds with N-Heterocyclic Carbene Ligands—Theoretical Evidence for a Class of Molecules with Promising Chemical Properties. *Angew. Chem., Int. Ed.* **2007**, *46*, 8695−8698.

(20) Dutton, J. L.; Wilson, D. J. D. Lewis Base Stabilized Dicarbon: Predictions from Theory. *Angew. Chem., Int. Ed.* **2012**, *51*, 1477−1480.

(21) Dyker, C. A.; Lavallo, V.; Donnadieu, B.; Bertrand, G. Synthesis of an Extremely Bent Acyclic Allene (a "Carbodicarbene"): A Strong Donor Ligand. *Angew. Chem., Int. Ed.* **2008**, *47*, 3206−3209.

(22) Wang, Y.; Xie, Y.; Wei, P.; King, R. B.; Schaefer, H. F.; von R. Schleyer, P.; Robinson, G. H. A Stable Silicon(0) Compound with a Si = Si Double Bond. *Science* **2008**, *321*, 1069−1071.

(23) Sidiropoulos, A.; Jones, C.; Stasch, A.; Klein, S.; Frenking, G. N-Heterocyclic Carbene Stabilized Digermanium(0). *Angew. Chem., Int. Ed.* **2009**, *48*, 9701−9704.

(24) Jones, C.; Sidiropoulos, A.; Holzmann, N.; Frenking, G.; Stasch, A. An N-Heterocyclic Carbene Adduct of Diatomic Tin, :Sn = Sn. *Chem. Commun. (Camb.)* **2012**, *48*, 9855−9857.

(25) Xiong, Y.; Yao, S.; Inoue, S.; Epping, J. D.; Driess, M. A Cyclic Silylone ("siladicarbene") with an Electron-Rich Silicon(0) Atom. *Angew. Chem., Int. Ed.* **2013**, *52*, 7147−7150.

(26) Xiong, Y.; Yao, S.; Tan, G.; Inoue, S.; Driess, M. A Cyclic Germadicarbene ("germylone") from Germyliumylidene. *J. Am. Chem. Soc.* **2013**, *135*, 5004−5007.

(27) Takagi, N.; Shimizu, T.; Frenking, G. Divalent Silicon(0) Compounds. *Chemistry* **2009**, *15*, 3448−3456.

(28) Takagi, N.; Shimizu, T.; Frenking, G. Divalent E(0) Compounds (E = Si−Sn). *Chemistry* **2009**, *15*, 8593−8604.

(29) Shan, Y.-L.; Yim, W.-L.; So, C.-W. An N-Heterocyclic Silylene-Stabilized Digermanium(0) Complex. *Angew. Chem., Int. Ed.* **2014**, *53*, 13155−13158.

(30) Mondal, K. C.; Roesky, H. W.; Schwarzer, M. C.; Frenking, G.; Niepötter, B.; Wolf, H.; Herbst-Irmer, R.; Stalke, D. A Stable Singlet Biradicaloid Siladicarbene: $(L:)_2Si$. *Angew. Chem., Int. Ed.* **2013**, *52*, 2963−2967.
(31) Li, Y.; Mondal, K. C.; Roesky, H. W.; Zhu, H.; Stollberg, P.; Herbst-Irmer, R.; Stalke, D.; Andrada, D. M. Acyclic Germylones: Congeners of Allenes with a Central Germanium Atom. *J. Am. Chem. Soc.* **2013**, *135*, 12422−12428.
(32) Soleilhavoup, M.; Bertrand, G. Cyclic (Alkyl)(Amino)Carbenes (CAACs): Stable Carbenes on the Rise. *Acc. Chem. Res.* **2015**, *48*, 256−266.
(33) Roy, S.; Mondal, K. C.; Roesky, H. W. Cyclic Alkyl(Amino) Carbene Stabilized Complexes with Low Coordinate Metals of Enduring Nature. *Acc. Chem. Res.* **2016**, *49*, 357−369.
(34) Meltzer, A.; Präsang, C.; Driess, M. Diketiminate Silicon(II) and Related NHSi Ligands Generated in the Coordination Sphere of Nickel(0). *J. Am. Chem. Soc.* **2009**, *131*, 7232−7233.
(35) Meltzer, A.; Inoue, S.; Präsang, C.; Driess, M. Steering S-H and N-H Bond Activation by a Stable n-Heterocyclic Silylene: Different Addition of H_2S, NH_3, and Organoamines on a Silicon(II) Ligand versus Its $Si(II)\rightarrow Ni(CO)_3$ Complex. *J. Am. Chem. Soc.* **2010**, *132*, 3038−3046.
(36) Jana, A.; Sarish, S. P.; Roesky, H. W.; Schulzke, C.; Samuel, P. P. A Rational Design for an Efficient Synthesis of a Monomeric Tin(II) Hydroxide. *Chem. Commun.* **2010**, *46*, 707−709.
(37) Jana, A.; Leusser, D.; Objartel, I.; Roesky, H. W.; Stalke, D. A Stable Silicon(II) Monohydride. *Dalton Trans.* **2011**, *40*, 5458−5463.
(38) Azhakar, R.; Ghadwal, R. S.; Roesky, H. W.; Wolf, H.; Stalke, D. Stabilization of Low Valent Silicon Fluorides in the Coordination Sphere of Transition Metals. *J. Am. Chem. Soc.* **2012**, *134*, 2423−2428.
(39) Zhang, S.-H.; Yeong, H.-X.; Xi, H.-W.; Lim, K. H.; So, C.-W. Hydrosilylation of a Silicon(II) Hydride: Synthesis and Characterization of a Remarkable Silylsilylene. *Chem. Eur. J.* **2010**, *16*, 10250−10254.
(40) Thimer, K. C.; Al-Rafia, S. M. I.; Ferguson, M. J.; McDonald, R.; Rivard, E. Donor/Acceptor Stabilization of Ge(II) Dihydride. *Chem. Commun.* **2009**, 7119−7121.
(41) Al-Rafia, S. M. I.; Malcolm, A. C.; Liew, S. K.; Ferguson, M. J.; Rivard, E. Stabilization of the Heavy Methylene Analogues, GeH_2 and SnH_2, within the Coordination Sphere of a Transition Metal. *J. Am. Chem. Soc.* **2011**, *133*, 777−779.
(42) Ibrahim Al-Rafia, S. M.; Malcolm, A. C.; Liew, S. K.; Ferguson, M. J.; McDonald, R.; Rivard, E. Intercepting Low Oxidation State Main Group Hydrides with a Nucleophilic N-Heterocyclic Olefin. *Chem. Commun.* **2011**, *47*, 6987−6989.
(43) Al-Rafia, S. M. I.; Malcolm, A. C.; McDonald, R.; Ferguson, M. J.; Rivard, E. Efficient Generation of Stable Adducts of Si(II) Dihydride Using a Donor-Acceptor Approach. *Chem. Commun.* **2012**, *48*, 1308−1310.
(44) Al-Rafia, S. M. I.; Shynkaruk, O.; McDonald, S. M.; Liew, S. K.; Ferguson, M. J.; McDonald, R.; Herber, R. H.; Rivard, E. Synthesis and Mössbauer Spectroscopy of Formal Tin(II) Dichloride and Dihydride Species Supported by Lewis Acids and Bases. *Inorg. Chem.* **2013**, *52*, 5581−5589.
(45) Swarnakar, A. K.; McDonald, S. M.; Deutsch, K. C.; Choi, P.; Ferguson, M. J.; McDonald, R.; Rivard, E. Application of the Donor-Acceptor Concept to Intercept Low Oxidation State Group 14 Element Hydrides Using a Wittig Reagent as a Lewis Base. *Inorg. Chem.* **2014**, *53*, 8662−8671.
(46) Al-Rafia, S. M. I.; Malcolm, A. C.; McDonald, R.; Ferguson, M. J.; Rivard, E. Trapping the parent inorganic ethylenes H_2SiGeH_2 and H_2SiSnH_2 in the form of stable adducts at ambient temperature. *Angew. Chem., Int. Ed.* **2011**, *50*, 8354−8357.
(47) Al-Rafia, S. M. I.; Momeni, M. R.; Ferguson, M. J.; McDonald, R.; Brown, A.; Rivard, E. Stable Complexes of Parent Digermene: An Inorganic Analogue of Ethylene. *Organometallics* **2013**, *32*, 6658−6665.
(48) Jana, A.; Huch, V.; Rzepa, H. S.; Scheschkewitz, D. A Molecular Complex with a Formally Neutral Iron Germanide Motif (Fe_2Ge_2). *Organometallics* **2015**, *34*, 2130−2133.
(49) Mandal, D.; Dhara, D.; Maiti, A.; Klemmer, L.; Huch, V.; Zimmer, M.; Rzepa, H. S.; Scheschkewitz, D.; Jana, A. Mono- and Dicoordinate Germanium(0) as a Four-Electron Donor. *Chem. Eur. J.* **2018**, *24*, 2873−2878.
(50) Zhou, Y.-P.; Karni, M.; Yao, S.; Apeloig, Y.; Driess, M. A Bis(Silylenyl)Pyridine Zero-Valent Germanium Complex and Its Remarkable Reactivity. *Angew. Chem., Int. Ed.* **2016**, *55*, 15096−15099.
(51) Xu, J.; Dai, C.; Yao, S.; Zhu, J.; Driess, M. A Genuine Stannylone with a Monoatomic Two-coordinate Tin(0) Atom Supported by a Bis(Silylene) Ligand. *Angew. Chem., Int. Ed.* **2022**, *61*, No. e202114073.
(52) Zhao, X.-X.; Szilvási, T.; Hanusch, F.; Kelly, J. A.; Fujimori, S.; Inoue, S. Isolation and Reactivity of Tetrylene-tetrylone-iron Complexes Supported by Bis(N-heterocyclic Imine) Ligands. *Angew. Chem., Int. Ed.* **2022**, *61*, No. e202208930.
(53) Xu, J.; Pan, S.; Yao, S.; Frenking, G.; Driess, M. The Heaviest Bottleable Metallylone: Synthesis of a Monatomic, Zero-Valent Lead Complex ("Plumbylone"). *Angew. Chem., Int. Ed.* **2022**, *61*, No. e202209442.
(54) Zybill, C.; Wilkinson, D. L.; Müller, G. Synthesis and Structure of $[(OC)_4Fe = Si = Fe(CO)_4 \cdot 2(Me_2N)_3PO]$-a Complex of Formally Zerovalent Silicon. *Angew. Chem., Int. Ed.* **1988**, *27*, 583−584.
(55) Budnikova, Y. G.; Gryaznova, T. V.; Sinyashin, O. G.; Katsyuba, S. A.; Gryaznova, T. P.; Egorov, M. P. Germylene complexes of tungsten pentacarbonyls $[W(CO)_5{=}GeCl_2]$ and $[W(CO)_5{=}Ge = W(CO)_5]$: Electrochemical synthesis and quantum-chemical computations. *J. Organomet. Chem.* **2007**, *692*, 4067−4072.
(56) Parameswaran, P.; Frenking, G. Transition-Metal Complexes $[(PMe_3)_2Cl_2M(E)]$ and $[(PMe_3)_2(CO)_2M(E)]$ with Naked Group 14 Atoms (E = C−Sn) as Ligands; Part 1: Parent Compounds. *Chem. Eur. J.* **2009**, *15*, 8807−8816.
(57) Parameswaran, P.; Frenking, G. Transition-Metal Complexes $[(PMe_3)_2Cl_2M(E)]$ and $[(PMe_3)_2(CO)_2M(E)]$ with Naked Group 14 Atoms (E = C−Sn) as Ligands; Part 2: Complexation with $W(CO)_5$. *Chem. Eur. J.* **2009**, *15*, 8817−8824.
(58) Jana, A.; Samuel, P. P.; Roesky, H. W.; Schulzke, C. Preparation of iron carbonyl complexes of germanium(II) and tin(II) each with a terminal fluorine atom. *J. Fluorine. Chem.* **2010**, *131*, 1096−1099.
(59) Jana, A.; Majumdar, M.; Huch, V.; Zimmer, M.; Scheschkewitz, D. NHC-coordinated silagermenylidene functionalized in allylic position and its behaviour as a ligand. *Dalton Trans.* **2014**, *43*, 5175−5181.
(60) Hickox, H. P.; Wang, Y.; Xie, Y.; Chen, M.; Wei, P.; Schaefer, H. F., III; Robinson, G. H. Transition-Metal-Mediated Cleavage of a Si = Si Double Bond. *Angew. Chem., Int. Ed.* **2015**, *54*, 10267−10270.
(61) Frisch, M. J.; Trucks, G. W.; Schlegel, H. B.; Scuseria, G. E.; Robb, M. A.; Cheeseman, J. R.; Scalmani, G.; Barone, V.; Mennucci, B.; Petersson, G. A.; Nakatsuji, H.; Caricato, M.; Li, X.; Hratchian, H. P.; Izmaylov, A. F.; Bloino, J.; Zheng, G.; Sonnenberg, J. L.; Hada, M.; Ehara, M.; Toyota, K.; Fukuda, R.; Hasegawa, J.; Ishida, M.; Nakajima, T.; Honda, Y.; Kitao, O.; Nakai, H.; Vreven, T.; Montgomery, J. A., Jr.; Peralta, J. E.; Ogliaro, F.; Bearpark, M.; Heyd, J. J.; Brothers, E.; Kudin, K. N.; Staroverov, V. N.; Kobayashi, R.; Normand, J.; Raghavachari, K.; Rendell, A.; Burant, J. C.; Iyengar, S. S.; Tomasi, J.; Cossi, M.; Rega, N.; Millam, J. M.; Klene, M.; Knox, J. E.; Cross, J. B.; Bakken, V.; Adamo, C.; Jaramillo, J.; Gomperts, R.; Stratmann, R. E.; Yazyev, O.; Austin, A. J.; Cammi, R.; Pomelli, C.; Ochterski, J. W.; Martin, R. L.; Morokuma, K.; Zakrzewski, V. G.; Voth, G. A.; Salvador, P.; Dannenberg, J. J.; Dapprich, S.; Daniels, A. D.; Farkas, O.; Foresman, J. B.; Ortiz, J. V.; Cioslowski, J.; Fox, D. J. Gaussian 09, Revision E.01; Gaussian, Inc.: Wallingford CT, 2016.
(62) Lee, C.; Yang, W.; Parr, R. G. Development of the Colle-Salvetti correlation-energy formula into a functional of the electron density. *Phy. Rev. B* **1988**, *37*, 785−789.

https://doi.org/10.1021/acs.jpca.3c04376
J. Phys. Chem. A 2023, 127, 9442−9450

(63) Becke, A. D. Density-functional thermochemistry. III. The role of exact exchange. *J. Chem. Phy.* **1993**, *98*, 5648−5652.
(64) Becke, A. D. Density-functional exchange-energy approximation with correct asymptotic behavior. *Phy. Rev. A* **1988**, *38*, 3098−3100.
(65) Vosko, S. H.; Wilk, L.; Nusair, M. Accurate spin-dependent electron liquid correlation energies for local spin density calculations: a critical analysis. *Journal of Physics* **1980**, *58*, 1200−1211.
(66) Dunning, T. H. Gaussian basis sets for use in correlated molecular calculations. I. The atoms boron through neon and hydrogen. *J. Chem. Phy.* **1989**, *90*, 1007−1023.
(67) Küchle, W.; Dolg, M.; Stoll, H.; Preuss, H. *Ab initio* pseudopotentials for Hg through Rn. *Mol. Phys.* **1991**, *74*, 1245−1263.
(68) Weinhold, F. Natural bond orbital analysis: A critical overview of relationships to alternative bonding perspectives. *J. Comput. Chem.* **2012**, *33*, 2363−2379.
(69) Glendening, E. D.; Landis, C. R.; Weinhold, F. NBO 6.0: Natural bond orbital analysis program. *J. Comput. Chem.* **2013**, *34*, 1429−1437.
(70) Bader, R. F. W. Atoms. In *Molecules: A Quantum Theory*; Clarendon: Oxford, 1990.
(71) The Quantum Theory of Atoms In *Molecules*; Matta, C. F., Boyd, R. J., Eds.; Wiley-VCH: Weinheim,2007.
(72) Becke, A. D.; Edgecombe, K. E. *J. Chem. Phys.* **1990**, *92*, 5397−5403.
(73) Keith, T. A. *AIMAll*, ver. 16.01.09; TK Gristmill Software: Overland Park KS, USA, 2016. aim.tkgristmill.com.
(74) Knizia, G. Intrinsic Atomic Orbitals: An Unbiased Bridge between Quantum Theory and Chemical Concepts. *J. Chem. Theory Comput.* **2013**, *9*, 4834−4843.
(75) Knizia, G.; Klein, J. E. Electron Flow in Reaction Mechanisms—Revealed from First Principles. *Angew. Chem., Int. Ed.* **2015**, *54*, 5518−5522.
(76) Lischka, H.; Köhler, H.-J. Ab initio investigation on the lowest singlet and triplet state of disilyne (Si_2H_2). *J. Am. Chem. Soc.* **1983**, *105*, 6646−6649.
(77) Grev, R. S.; Dee Leeuw, B. J.; Schaefer, H. F. Germanium-germanium multiple bonds: The singlet electronic ground state of Ge_2H_2. *Chem. Phys. Lett.* **1990**, *165*, 257−264.
(78) Palagyi, Z.; Schaefer, H. F.; Kapuy, E. Ge_2H_2: a germanium-containing molecule with a low-lying monobridged equilibrium geometry. *J. Am. Chem. Soc.* **1993**, *115*, 6901−6903.
(79) Nagase, S.; Kobayashi, K.; Takagi, N. Triple bonds between heavier Group 14 elements. A theoretical approach. *J. Organomet. Chem.* **2000**, *611*, 264−271.
(80) Lein, M.; Krapp, A.; Frenking, G. Why Do the Heavy-Atom Analogues of Acetylene E_2H_2 (E = Si−Pb) Exhibit Unusual Structures? *J. Am. Chem. Soc.* **2005**, *127*, 6290−6299.
(81) Trinquier, G. Double bonds and bridged structures in the heavier analogs of ethylene. *J. Am. Chem. Soc.* **1990**, *112*, 2130−2137.
(82) Schreiner, P. R.; Chernish, L. V.; Gunchenko, P. A.; Tikhonchuk, E. Yu.; Hausmann, H.; Serafin, M.; Schlecht, S.; Dahl, J. E. P.; Carlson, R. M. K.; Fokin, A. A. Overcoming lability of extremely long alkane carbon−carbon bonds through dispersion forces. *Nature* **2011**, *477*, 308−312.
(83) Power, P. P. Silicon, germanium, tin and lead analogues of acetylenes. *Chem. Commun.* **2003**, 2091−2101.
(84) Kutzelnigg, W. Chemical Bonding in Higher Main Group Elements. *Angew. Chem., Int. Ed. Engl.* **1984**, *23*, 272−295.
(85) Lee, V. Y.; Sekiguchi, A. *Organometallic Compounds of Low-Coordinate Si, Ge, Sn, and Pb: From Phantom Species to Stable Compounds*; John Wiley & Sons, Ltd., 2010; Chapter 5, pp 199-334.
(86) Pietschnig, R.; West, R.; Powell, D. R. Reduction of Terphenyltrifluorosilanes: C−C Insertion Products and Possible Formation of a Disilyne. *Organometallics* **2000**, *19*, 2724−2729.

https://doi.org/10.1021/acs.jpca.3c04376
J. Phys. Chem. A 2023, 127, 9442−9450